The Role of Katabatic Winds on the Antarctic Surface Wind Regime

THOMAS R. PARISH

Department of Atmospheric Science, University of Wyoming, Laramie, Wyoming

JOHN J. CASSANO

Cooperative Institute for Research in Environmental Sciences, University of Colorado, Boulder, Colorado

(Manuscript received 22 March 2001, in final form 15 October 2001)

ABSTRACT

Antarctica is known for its strong and persistent surface winds that are directed along topographic pathways. Surface winds are especially strong during the winter period. The high directional constancy of the wind and the close relationship of the wind direction to the underlying terrain can be interpreted as evidence of katabatic wind activity. Observations show that the directional constancy of the Antarctic surface wind displays little seasonal variation. Summertime winds cannot be expected to contain a significant katabatic component, owing to enhanced solar heating of the ice slopes. Observations also show that the coastal environs are subjected to wide variation in atmospheric pressure associated with frequent cyclone activity. The robust unidirectional nature of the Antarctic surface wind throughout the year implies that significant topographic influences other than those from katabatic forcing must be acting.

Idealized numerical simulations have been performed to illustrate the potential role of the Antarctic topography in shaping the wind. The presence of katabatic winds is dependent on radiative cooling of the ice slopes. Simulations without explicit longwave radiation show that the blocking influence of the Antarctic orography is a powerful constraint to the surface wind regime. Resulting low-level wind fields resemble katabatic winds, with directions being tied to the underlying terrain and speeds dependent on the slope of the ice surface. A numerical simulation of a strong wind event during austral autumn shows that the katabatic component is only a small fraction of the horizontal pressure gradient force for this case. This suggests that the role of katabatic winds in the Antarctic boundary layer may be overemphasized and that the adjustment process between the continental ice surface and the ambient pressure field may be the primary cause of the Antarctic wind field.

1. Introduction

The term ''katabatic'' has been applied to a variety of atmospheric flows in the meteorological literature. A review of selected popular texts on meteorology reveals differences in how a katabatic wind is viewed. For example, Ahrens (2000) provides the following definition of a katabatic wind: ''Any wind blowing downslope. It is usually cold.'' Lutgens and Tarbuck (2001) offer that a katabatic wind is defined as a ''flow of cold dense air downslope under the influence of gravity; the direction is controlled largely by topography.'' Moran and Morgan (1997) give a similar definition. Huschke's *Glossary of Meteorology* (1959) specifies two definitions of a katabatic wind: 1) ''any wind blowing down an incline'' and 2) ''a 'gravity wind,' that is, a wind directed down the slope of an incline and caused by greater air density near the slope than at the same levels some distance horizontally from the slope.'' As noted by Schwerdtfeger (1970), the ambiguity surrounding katabatic winds permits a broad spectrum of topographic winds to be categorized as ''katabatic.''

Use of katabatic as it applies to the surface winds over Antarctica is somewhat more restrictive. Ball (1956) notes that katabatic is applied to ''winds which blow down slopes that are cooled by radiation,'' implying the second definition in Huschke (1959). The negatively buoyant nature of katabatic winds has been implied in papers that follow Ball's original presentation (e.g., Ball 1960; Mather and Miller 1966, 1967; Lettau and Schwerdtfeger 1967; Schwerdtfeger 1970, 1984; Radok 1973) and will be adopted here. Using this definition, katabatic winds are colder than the air displaced during the downslope descent and are not dependent on the orientation of the large-scale horizontal pressure gradient force (PGF) in the free atmosphere for their origin.

Antarctic surface winds are among the most persistent on Earth. Wind directional constancy, a ratio of the resultant wind speed to the mean wind speed, is a useful measure of persistence. A directional constancy of 1.0 implies unidirectional flow; a directional constancy of 0.0 implies wind components of equal strength from all

Corresponding author address: Thomas R. Parish, Dept. of Atmospheric Science, University of Wyoming, Laramie, WY 82071.
E-mail: parish@uwyo.edu

sectors. Resultant wind statistics, such as those shown in Parish (1982) for historical sites or in Keller et al. (1994) for the more recently deployed automatic weather stations (AWSs), indicate that mean monthly directional constancies for Antarctic surface winds typically exceed 0.90 over all but the most gentle slopes of the Antarctic continent. Given the strong topographic control of the surface winds and geographic location of Antarctica, it would be logical to infer that the time-averaged winds are primarily katabatic in origin. In practice, however, it is difficult to categorize Antarctic winds as katabatic or nonkatabatic as defined following Ball (1956). Surface observations often are insufficient to determine the buoyancy of the flow. Temperature change alone is unreliable since katabatic winds tend to induce vertical mixing, thus destroying shallow low-level inversions. It is not uncommon that the onset of strong drainage flows is accompanied by a surface temperature increase. In addition, the coastal environment of Antarctica is one of the most active baroclinic zones on the planet. Surface winds thus are the result of the combined influence of katabatic and synoptic influences (e.g., Murphy and Simmonds 1993; Simmonds 1998; Parish and Cassano 2001).

The purpose of this paper is to examine the relationship between the Antarctic surface wind regime and horizontal pressure gradients in the free atmosphere. In particular, emphasis will be placed on the role of the Antarctic topography in shaping the low-level wind field without regard to katabatic influences. Section 2 depicts observational evidence of the strong topographic control of the Antarctic surface wind regime near the continental coastal margin. Idealized numerical simulations of synoptic processes along the Antarctic periphery and their effects on the wind field over Antarctica are presented in section 3. A brief case study emphasizing the surface wind field will be presented in section 4 and a summary is included in section 5.

2. Observations of the Antarctic surface wind regime

Surface wind observations testify to the first-order importance of the Antarctic topography on the low-level wind field. Previous results (e.g., Mather and Miller 1967; Parish 1982; Wendler and Kodama 1985; Keller et al. 1994) leave no doubt as to the overwhelming topographic control over the Antarctic low-level wind regime.

Documentation of the surface wind regime during the past two decades has been enhanced significantly with the deployment of arrays of AWSs. Figure 1 depicts an example of the strong topographic forcing of Antarctic surface winds, illustrating wind statistics from the AWS at the coastal station Cape Denison (67.1°S, 142.7°E). The data are taken for the year 1995, which contains the most complete record for this station. AWS observations are taken at 3-hourly intervals. Figure 1a shows the frequency of the wind direction for the entire year. It can be seen that the vast majority of wind direction observations were from a narrow range centered about SSE. Cape Denison had a resultant wind of 20.9 m s^{-1} from 162° with a directional constancy of 0.96 for the entire year 1995. The fall line, the line of action of the terrain gradient pointing down the slope, is directed 180° implying that the resultant wind is deflected at an angle approximately 20° to the left of downslope. These statistics match well with historical records at this station (Parish 1982). From Fig. 1a, it can be seen that over 80% of the 1995 wind observations are from directions between 135° and 195°. Inspection of the 1995 AWS records shows that the wind is directed with an upslope component infrequently. Out of a total of 2273 observations (647 observations are missing), only 79, or 3%, of the 3-hourly reports indicate an upslope component. Out of those cases, it was usually observed that upslope components did not persist longer than one observing period. The longest consecutive period with upslope conditions was found on December 11 over the 6-h period from 0600 to 1200 UTC.

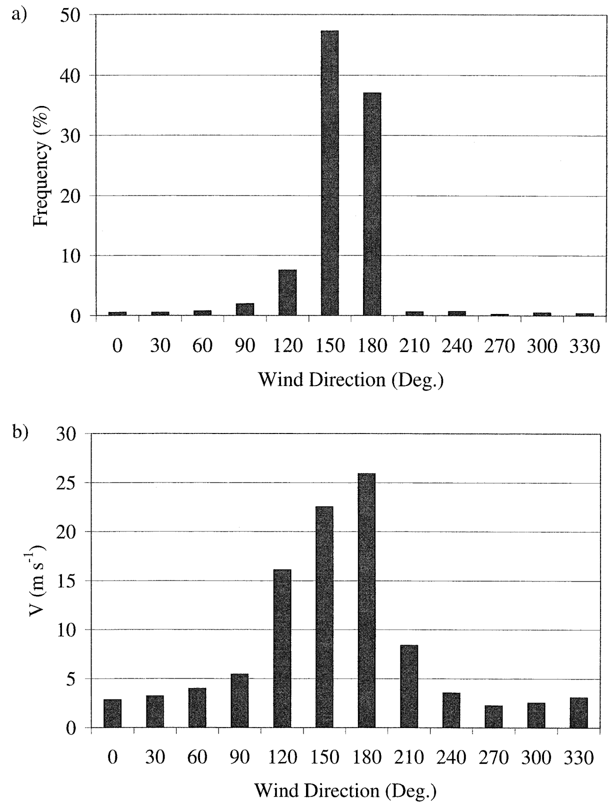

FIG. 1. Histograms showing the (a) wind direction frequency and (b) directional frequency of wind speed based on 1995 AWS 3-hourly records for Cape Denison.

AWS data for Cape Denison also reveal a marked directional preference in the intensity of the wind. Figure 1b illustrates the mean wind speed for 30° classes of wind direction. The magnitude of the wind along the preferred topographic pathways centered about 150° and 180° is approximately 25 m s^{-1}. Mean wind speeds at other directions are generally less than 5 m s^{-1}. Examination of the wind record shows that wind speeds in excess of 10 m s^{-1} are present only along the downslope direction. The Cape Denison wind regime is the most intense ever recorded at a site near sea level. Although the mean strength of the wind surpasses that at other Antarctic coastal stations, the directional preference and wind characteristics shown at Cape Denison are representative of the low-level wind environment over the continental ice slopes.

Given this extreme directional preference of the surface wind at coastal stations about the Antarctic rim such as Cape Denison, it is appropriate to inquire as to why this is so. Prolonged conditions of strong radiative cooling during winter months will prompt significant katabatic wind activity. These katabatic winds would be expected to match observed characteristics of Antarctic winds such as the directional preference to topographic features and the intensity of the flow dependent on terrain slope. During summer months from December through February and even at times during transitional months, solar insolation disrupts surface cooling. Katabatic wind episodes should decrease in frequency and intensity in response to the diabatic heating. AWS data for Cape Denison confirm a weaker surface wind regime during summer. Kodama et al. (1989) conducted a summer field program near Cape Denison and noted that a pronounced diurnal cycle is present. Only weak or nonexistent katabatic flow can be expected from midmorning through late afternoon during summer as a result of the initial temperature profiles during summer. Resultant wind statistics for December, January, and February (DJF) 1995 at Cape Denison confirm the weaker summer surface winds. The resultant wind speed for the three summer months amounted to 14.2 m s^{-1} as compared to 23.4 m s^{-1} for the months June, July, and August 1995. DJF wind speeds showed a distinct diurnal variation similar to that noted by Kodama et al. (1989) with a minimum (10.7 m s^{-1}) in the afternoon (0600 UTC) and maximum (17.2 m s^{-1}) in the early morning (1800 UTC). Mean wind directions showed little seasonal variation, ranging from 157° during summer to 161° during winter. There was a consistent diurnal variation during the DJF period with a mean direction of 150° at 0600 UTC and 162° at 1800 UTC. The DJF directional constancy value of 0.94 was nearly identical to those for the entire year. Inspection of the wind constancy during the summer months revealed only a small diurnal cycle. Values in excess of 0.90 were found even during the summertime afternoon period. This implies that the surface wind at Cape Denison is nearly unidirectional throughout both summer and winter periods. It is clear that the summertime wind, although not as intense, still retains a close relationship to the underlying terrain. The fact that the wind retains such a high degree of organization about the topography implies that factors other than katabatic forcing are at work to shape the summertime wind field.

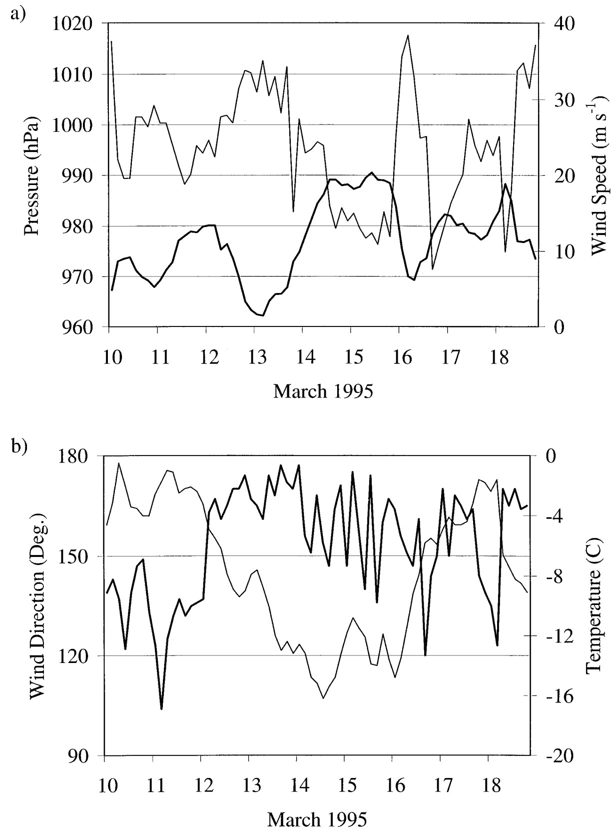

FIG. 2. Time series of (a) pressure (hPa, thick line) and wind speed (m s^{-1}, thin line), (b) wind direction (°, thick line) and temperature (°C, thin line) for the Cape Denison AWS for 10–19 Mar 1995.

A strong baroclinic zone exists about the Antarctic continent throughout much of the year. As a result, the coastal margin is one of the most active cyclogenetic regions on earth. As noted by Simmonds (1998), the greatest density of cyclones in the entire Southern Hemisphere is found just north of the Antarctic coastline. Turner et al. (1998) report that over half of the cyclones adjacent to the continent near the Antarctic Peninsula had experienced cyclogenesis within that general region. Schwerdtfeger (1984) pointed out that the coastal section of Antarctica near Cape Denison has experienced a range in atmospheric pressure in excess of 100 hPa, illustrating the intensity of cyclonic events in this region. Highest cyclone densities adjacent to Antarctica occur during the transitional seasons of spring and autumn (e.g., Schwerdtfeger 1984; Simmonds 1998). Given the active cyclonic environment along the coastal margins of Antarctica, it follows that the horizontal pressure fields accompanying such disturbances must play a role in the surface wind field (Neff 1999).

As an illustration of the cyclonic influence on the coastal environment, Fig. 2 shows a time series of surface pressure, wind speed, wind direction, and temperature from the Cape Denison AWS data during the period 11–19 March 1995. As can be seen in Fig 2a, two cyclonic disturbances passed to the north of Cape Denison during this 9-day period. The first trough axis passed Cape Denison at approximately 0000 UTC 13 March and the second around 0600 UTC 16 March. Significant ridging occurred between the cyclonic events. Surface pressure rose in excess of 25 hPa in a 36-h interval commencing early on 13 March. Examination of the wind speeds at Cape Denison clearly shows the influence of the cyclonic events on the intensity of the wind. The wind speeds are negatively correlated with surface pressure with maximum winds seen near the time of minimum pressure. This suggests that the synoptic environment is responsible for forcing a significant component of the surface wind. Wind directions (Fig. 1b) maintain a downslope component throughout the entire period. Only modest wind direction changes accompany passage of the initial cyclone, and little change in wind direction occurs during the subsequent ridging period and approach of the second cyclone. Ball (1960) has also noted that small directional changes are present in the surface wind accompanying cyclonic events. This is evidence of the robust nature of the wind direction in the low levels over the Antarctic continent. Coldest surface temperatures are seen during the period of ridging from 14 to 16 March and are associated with weaker winds although the correlation between wind speed and temperature is not significant. Temperature is a poor indicator of wind speed or presence of katabatic activity.

3. Idealized simulations of the Antarctic surface winds

A series of numerical simulations were conducted to examine the role of the Antarctic topography on the wind field in the lowest layers of the atmosphere. In particular, the simulations were designed to explore processes by which the flows over the steep Antarctic coastal sections could be directed down observed topographic pathways. The fifth-generation Pennsylvania State University–National Center for Atmospheric Research Mesoscale Model (MM5) was used for all simulations. Detailed description of MM5 can be found in Grell et al. (1994). Following the work of Cassano and Parish (2000), the hydrostatic form of version 2.9 is used. This allows comparison with results of older model studies (e.g., Parish and Waight 1987) since MM5 version 3 has no hydrostatic option.

As in Cassano and Parish (2000), the model simulations are for dry processes only and effects of latent heating are neglected. The simulations are valid for winter conditions. No solar insolation is considered in the simulations. The Medium Range Forecast (MRF) model scheme (Hong and Pan 1996) is used to simulate fluxes in the planetary boundary layer (PBL); the Community Climate Model 2 (CCM2) parameterization (Hack et al. 1993) is used to simulate the long- and shortwave radiation fluxes. Zero-gradient lateral boundary conditions were used for both horizontal directions. Sensitivity experiments have been conducted with MM5 using a variety of boundary layer parameterizations, which for brevity are not presented. The general conclusions reached in this section are not dependent on the hydrostatic assumption or the particular choice of PBL model parameterizations.

The topographic representation of Antarctica follows that of Parish and Waight (1987) and Cassano and Parish (2000). The model domain consists of a section 800 km inland of the Antarctic continent and 400 km over the assumed ice-covered ocean. A 20-km grid spacing was used in all experiments. In the vertical, 25 sigma levels were specified with the lowest level approximately 11 m above the surface over the Antarctic terrain. Seven sigma levels were located within the lowest 250 m to depict details of the near-surface wind and temperature fields. The model topography is based on a cross section of Antarctic terrain along 90°E. Sinusoidal lateral terrain variations were superimposed on the meridional terrain profile to replicate topographic features observed in parts of East Antarctica. All simulations were initialized with a temperature profile based on the sounding in Schwerdtfeger (1984, his Fig. 6.9) that is representative of winter conditions over the interior. The initial temperature profile did not incorporate the strong inversion in the lower atmosphere and hence no katabatic acceleration was present at the start of the model runs. Simulations were carried out for a 12-h period by which time the flows had adjusted to a quasi-steady state. For brevity, emphasis will be placed on the winds at the lowest sigma level since historical station records and AWS observations emphasize surface values.

To begin, a control katabatic wind experiment was conducted in which MM5 is initialized about a state of rest (case CR). A uniform zero PGF is specified so as to isolate katabatic effects. Longwave radiative flux divergence acts to cool the surface and the overlying lowest layers of the atmosphere, producing a negatively buoyant layer of air adjacent to the ice surface. This results in the establishment of a PFG near the surface that is responsible for the downslope acceleration of the wind. Figure 3 illustrates the wind vectors at the lowest sigma level at 0, 3, 6, and 12 h for CR. Spinup time for the katabatic wind regime requires at least 6 h although flows are quasi steady by 12 h. Katabatic winds are strongest over the steeply sloping coastal ice slopes with speeds in excess of 20 m s^{-1} after 12 h. The sinusoidal undulations in the ice topography disrupt significantly the drainage pattern near the surface such that convergence of the drainage flow is present along the left side of topographic depressions in CR. Such ''confluence zones'' are present at various sites over the Antarctic continent (e.g., Ball 1960; Parish and Bromwich 1987) and have been identified as the reason for the anomalous intensity of the Cape Dension wind (Parish

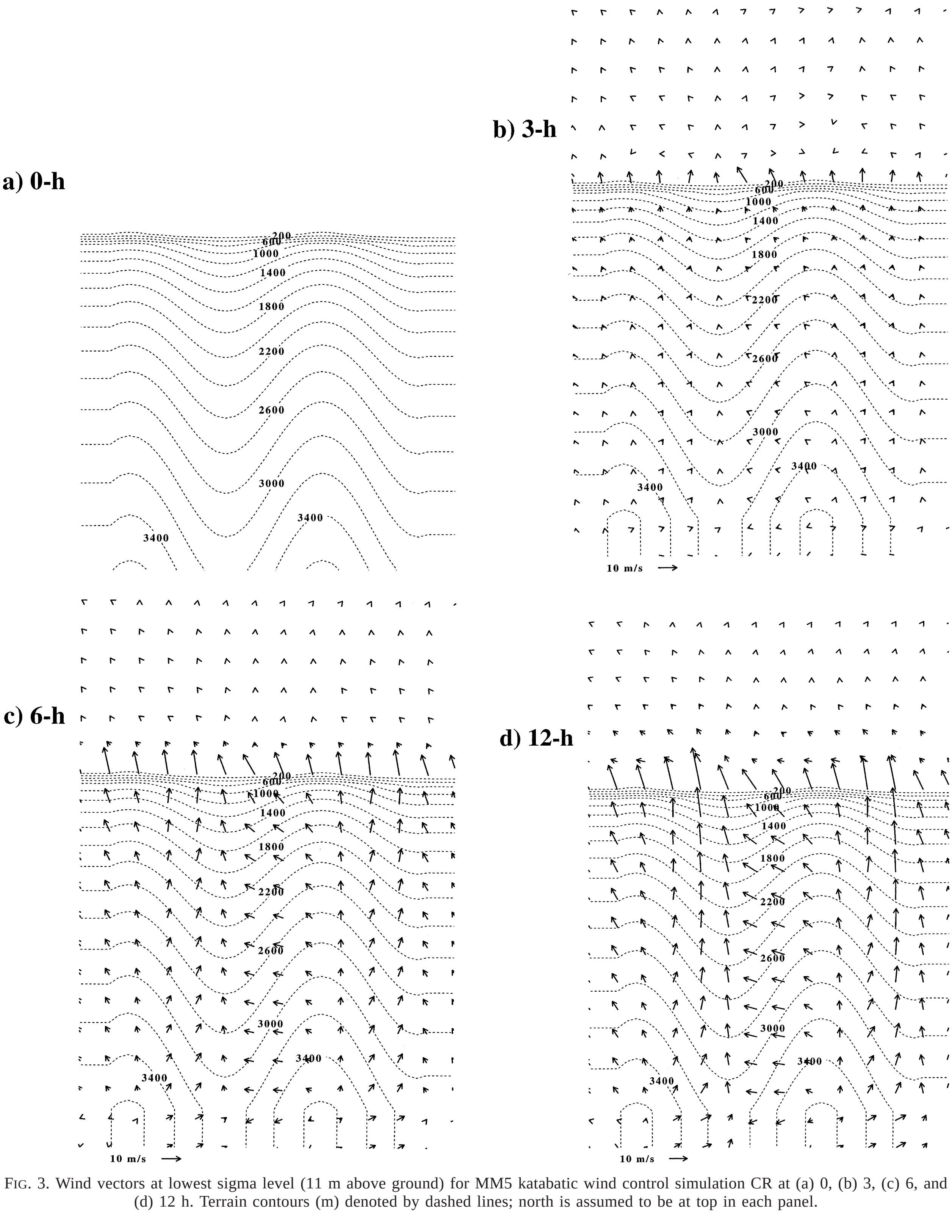

FIG. 3. Wind vectors at lowest sigma level (11 m above ground) for MM5 katabatic wind control simulation CR at (a) 0, (b) 3, (c) 6, and (d) 12 h. Terrain contours (m) denoted by dashed lines; north is assumed to be at top in each panel.

1981; Parish and Wendler 1991). Wind speeds at the coast at 12 h in CR vary from approximately 12 to 22 m s^{-1} depending on proximity to the confluence zone, illustrating the profound influence that the ice terrain has on the intensity of the wind. Wind directions of the katabatic flow are directed 20°–40° to the left of the fall line, consistent with Coriolis deflection of gravity-driven flows. The katabatic regime simulated by CR as shown in Fig. 3 is in good agreement with surface observations over Antarctica in terms of wind speed and direction for both the ''ordinary'' katabatic-prone stations and ''extraordinary'' sites such as Cape Denison (Schwerdtfeger 1984).

Given that the Antarctic surface wind regime retains its directional preference during nonwinter periods, it is apparent that the topography controls the surface wind through other means than the katabatic process. The mean low-level PGF in the ambient atmosphere near the coast of Antarctica is directed toward the north (e.g., Schwerdtfeger 1984; Kodama et al. 1989). A circumpolar trough of low pressure persists to the north of the continent throughout the year. Schwerdtfeger (1984) and Simmonds (1998) note that the position of the circumpolar trough varies seasonally and is tied to the semiannual oscillation of pressure (e.g., Schwerdtfeger 1960; van Loon 1967; Meehl 1991). The closest approach of the circumpolar trough to the continent occurs during the equinox periods. Specification of the ambient pressure field over the Antarctic is complicated by the ice topography. Reduction of pressure to sea level is often meaningless over the high plateau and consequently analyses of sea level pressure have a high degree of uncertainty. There seems little doubt, however, that the ambient PGF is directed north.

Simulations have been performed assuming a uniform PGF directed north over the idealized continent. To eliminate effects of the katabatic wind, the CCM2 radiation parameterization was inactivated. As a means of checking that no katabatic effects are present, 12-h simulations were first conducted about an initial state of rest. This should result in a motionless final state since there is no mechanism to produce a PGF. At the end of this test simulation (not shown), no katabatic wind regime developed during the period and the motion field remained calm with just minor wind components (less than 2 m s^{-1}) developing at the grid point corresponding to the terminal ice slope. With the knowledge that no significant katabatic components could form in the absence of the longwave radiation, simulations were run with a variety of prescribed PGF conditions. All simulations were initialized with a uniform PGF directed to the north at all levels. An example, which is presented here, consists of a PGF equivalent to an easterly geostrophic wind of 20 m s^{-1} at all levels (case SF). This implies a horizontal pressure gradient with higher pressures over the continent. Wind components to start the simulation were set to their geostrophic values at all levels. Figure 4 shows the wind vectors at the lowest sigma level at 0, 3, 6, and 12 h for the SF simulation. A rapid adjustment of the wind field takes place over the continent during the first few hours and the surface wind field shows the influence of irregularities in the underlying terrain. As stable air becomes forced against elevated terrain, such as occurs along the western side of the topographic troughs, the flow decelerates and becomes dammed up against the terrain. This results in an increase in the pressure and a modification of the PGF over the continent. An adjustment occurs such that the PGF becomes directed locally downslope at each grid point. The adjustment process as described here is the same as that discussed in Schwerdtfeger (1975) under the general topic of ''barrier winds.'' Bintanja (2000) has also addressed the development of barrier winds based on observations over the Antarctic continent. Adjustment continues such that by 12 h the wind field over the continent is directed along favored topographic pathways similar to that of a katabatic wind regime. Examination of the wind field again reveals a pronounced confluence zone. Wind speeds at 12 h along the coastline in SF vary from 20 m s^{-1} downwind of the confluence zones to less than 12 m s^{-1} downslope of the topographic ridge features, similar to those speeds seen in the katabatic control case of Fig. 3. The lowest-level wind field in SF is qualitatively and quantitatively similar to CR. This points out the difficulty in categorizing Antarctic flows from surface data alone. It should be noted that specification of the magnitude of the initial PGF is not critical to the development of the wind regime shown in Fig. 4b. Similar experiments were conducted with initial easterly geostrophic winds of 5 and 10 m s^{-1} that resulted in a wind field with comparable spinup times for the flows and nearly identical directions and similar magnitudes at 12 h. These experiments are analogous to the rotating tank experiments described by Baines and Fraedrich (1989). In that work, a tendency of the flow to follow the topographic contours was noted as well and it was concluded that atmospheric flow patterns are forced by the Antarctic topography.

Differences between SF and CR become obvious with inspection of the vertical profiles of wind, temperature, and PGF. Figure 5 illustrates the vertical structure in the lowest 3000 m for both cases at a coastal grid point at an elevation of approximately 600 m, situated over the steep slopes within the confluence zone. Wind speeds (Fig. 5a) depict a jet profile and low-level maximum for both SF and CR. A rapid decrease in the wind speed with height is present in CR such that only weak winds are observed above the katabatic layer. Wind speeds in SF remain in excess of 10 m s^{-1} throughout the lower atmosphere and increase to their geostrophic values in the upper levels in response to the initial PGF. Differences in the forcing of the wind in CR and SF can also be seen from the temperature profiles (Fig. 5b). A pronounced inversion is seen in CR as expected, implying a local forcing of the wind by katabatic processes. The temperature profile for SF in the lowest 200 m is con-

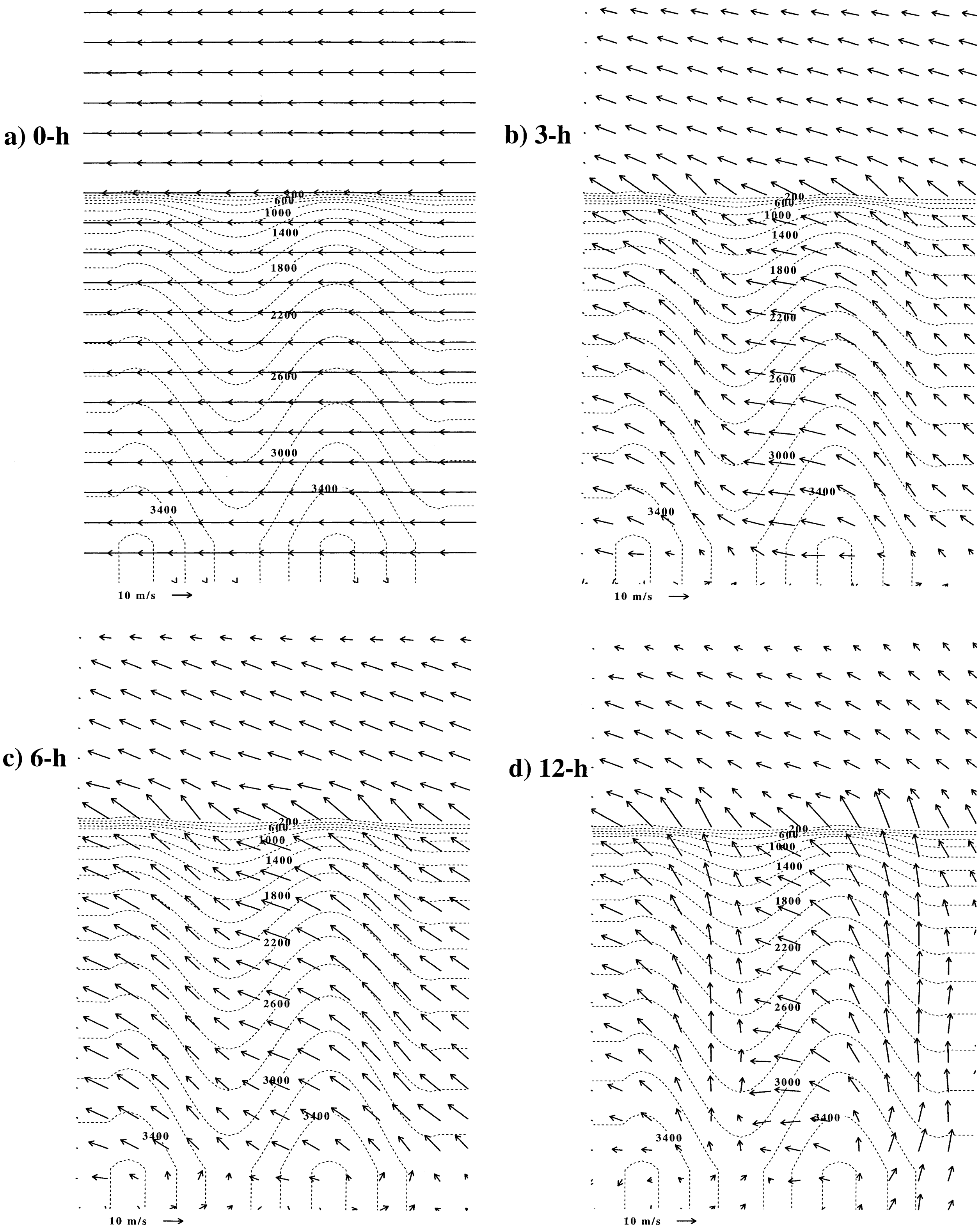

FIG. 4. As in Fig. 3 except for the MM5 synoptic force case (SF) with initial uniform 20 m s^{-1} easterly geostrophic winds at all levels.

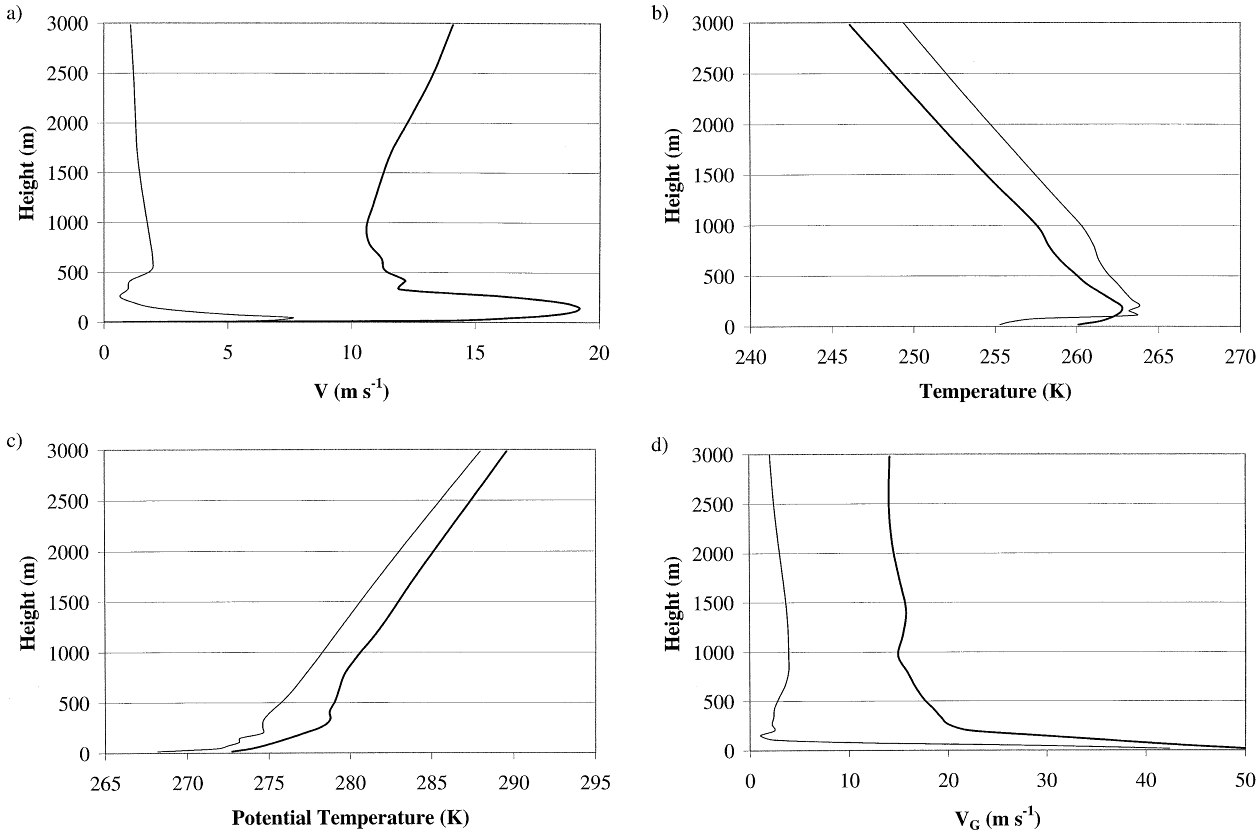

FIG. 5. Vertical profiles of (a) wind speed (m s^{-1}), (b) temperature (°C), (c) potential temperature (K), and (d) geostrophic winds (m s^{-1}) after 12-h model simulation for CR (thin line) and SF (thick line) experiments.

siderably different and only a weak inversion is present in the lowest layers that must arise as part of the adjustment process.

Examination of the potential temperature profile (Fig. 5c) reveals more clearly the fundamental forcing differences in CR and SF. The negatively buoyant nature of the katabatic wind in CR is apparent. As noted in Parish and Cassano (2001), the PGF in the katabatic layer can be approximated by

$$\mathrm{PGF} = g\frac{d}{\Theta_0}\sin\alpha - \frac{1}{\rho}\frac{\partial p}{\partial s_{\mathrm{syn}}}, \qquad (1)$$

where d is the potential temperature deficit, the difference in potential temperature at any point in the katabatic layer between the radiatively cooled layer and the ambient atmosphere. The term α refers to the terrain slope, Θ_0 is the mean potential temperature in the cooled layer, and s refers to a horizontal distance. Other symbols have their usual meteorological meaning. The first rhs term is the katabatic force, arising due to radiative cooling of the ice slopes and hence a temperature deficit over sloping terrain. The second rhs term is due to the PGF in the free atmosphere above the layer of diabatic cooling. As shown in Parish and Cassano (2001), the potential temperature deficit, d, at each level can be obtained by fitting a line to the potential temperature profile in the free atmosphere. Extrapolation of this line to the surface provides an estimate of the ambient thermal structure. The potential difference between the radiatively cooled near-surface layer and the ambient environment yields d.

In Fig. 5c the ambient profile can be estimated by linear extrapolation of the potential temperature profile between 1000 and 3000 m to the surface. This indicates that the potential temperature deficits at the lowest sigma level for CR and SF are approximately 9 and 1.5 K, respectively. From the first rhs term in (1), the PGF at this point should be equivalent to a geostrophic wind of about 49 m s^{-1} for CR and less than 10 m s^{-1} for SF. Such estimates can be compared with the PGF simulated from MM5. Figure 5d illustrates the profiles of the PGF in the MM5 simulations for CR and SF at the same grid point. Values are expressed in terms of the geostrophic wind. Note that at the first sigma level, the geostrophic wind exceeds 40 m s^{-1} in both simulations. The magnitude of the PGF in CR is well approximated by the first term in (1). In SF the total PGF is controlled by the second term in (1), indicating that it is the adjusted PGF owing to the combined effect of the initial PGF and blocking of stable air that is responsible for the forcing of the wind rather than diabatic cooling processes. The important point in this comparison is that although the near-surface wind field is quantitatively similar in CR and SF, the forcing mechanisms differ markedly.

Numerical experiments were also conducted to explore the blocking influence of the Antarctic terrain on ambient flows directed perpendicular to the ice sheet. Simulations were again initialized about a uniform geostrophic wind at all levels directed at the continent. As before, the effects of longwave radiation have been eliminated from this simulation so the katabatic wind regime cannot become established during the integration period. The evolving wind fields are the result of blocking effects only. The impulsive start to the simulation may be interpreted as what may occur as an intense cyclone impinges on the coastal escarpment. The example shown is for geostrophic wind conditions of 10 m s^{-1} directed at the Antarctic ice sheet (case BF). This corresponds to a PGF that is directed to the west, oriented such that isobars are perpendicular to the principal orientation of the terrain. As before, the simulation was carried out for a 12-h model integration period.

Figure 6 shows the BF wind vectors at the lowest sigma level for 0, 3, 6, and 9 h, covering the period of most significant adjustment. As seen previously, a pronounced and rapid adjustment in the PGF occurs within the first few hours. As the stable air impinges on the steep continental ice slopes, deceleration and piling up of the flow along the ice slopes takes place. The pressure rises owing to the blocking effect adjacent to the terrain, and the horizontal pressure field becomes modified. The adjusted PGF becomes directed to the north. This is illustrated by the changes in the low-level wind. By 3 h, the wind directions in BF at the lowest sigma level near the coast have switched from the initial northerly direction to southerly. At 6 h, the flow takes on characteristics of katabatic flow, being controlled by the slope and orientation of the local terrain. Strongest winds are found over the steep coastal section with speeds of approximately 20 m s^{-1}. Note that the PGF has been modified to the north of the continent due to the pronounced mass adjustment. The vector winds at 9 h in BF are similar to the katabatic wind fields of CR. This extreme example of blocking shows that the adjustment process between the wind and pressure fields over the Antarctic continent produces flows that become shaped by the orientation and slope of the terrain. Simulations were also conducted for initial geostrophic winds of 2.5, 5, and 20 m s^{-1} directed onto the Antarctic ice sheet, which produced similar results.

Given the overwhelming influence that the Antarctic topography plays in establishing the wind field in the lowest levels of the atmosphere, it is no wonder that the observed surface winds display such persistence. The lesson to be learned from the preceding simulations is that the surface wind over the continent may be forced by a number of different processes. These include 1) horizontal pressure gradients arising from the general circulation of the atmosphere at high latitudes, 2) blocking phenomena associated with cyclonic circulations in the vicinity of the continental ice slopes, and 3) the radiative cooling of the ice slopes to produce a katabatic force. It should not be assumed that the wind is katabatic merely because surface flows follow preferred topographic pathways. Wind direction is a poor indicator as to the katabatic nature of Antarctic surface winds.

4. Forcing of the surface winds during the cyclonic event of 11–15 March 1995

A major cyclone passed to the north of Cape Denison on 13 March 1995 as can be seen from the AWS data in Fig. 2. Wind speeds as recorded by the AWS (Fig. 2a) increased from 20 to 35 m s^{-1} as the storm approached. Figure 7 illustrates the sea level pressure maps for 0000 UTC 12 and 13 March 1995 based on analyses from the National Centers for Environmental Prediction–National Center for Atmospheric Research (NCAR–NCAR) 40-Year Reanalysis Project (Kalnay et al. 1996) to show the progression of the cyclone. The cyclone intensified considerably during the 24-h period with the central pressure decreasing by 12 hPa. It appears as though the PGF on the south side of the cyclone increased significantly as the storm deepened and impinged on the continental orography. The focus here is to examine the forcing of the wind associated with this cyclonic event and to determine the relative roles of ambient and katabatic components of the PGF in forcing the surface wind. For brevity, only the lowest-level wind and PGF components are presented.

A numerical simulation of this event was conducted using the nonhydrostatic version of MM5 version 2.9. The integration period was from 0000 UTC 12 March to 0000 14 March 1995. Initial grids were taken from the NCEP–NCAR reanalysis for 0000 UTC 12 March 1995. The model domain consists of a horizontal grid of 61 by 61 points with a grid spacing of 60 km and a vertical grid with 25 levels. To better compare with the AWS records, the lowest level in this simulation was set at approximately 5 m above the surface over the continent. As before, the highest vertical resolution is found in the boundary layer with seven levels below 250 m. Both the MRF boundary layer parameterization and CCM2 radiation scheme are used in the simulation and thus the effects of katabatic forcing are possible in this simulation. Unlike the idealized experiments described in the previous section, moist processes were considered in this simulation and thus clouds and precipitation could develop.

Figure 8 illustrates the MM5 wind vectors at the lowest sigma level at 12-h intervals for the simulation beginning at 0000 UTC 12 March 1995. Consistent with AWS observations at Cape Denison, the wind maintains a close relationship with the underlying terrain throughout the period, despite the strong forcing from the cyclone. Wind vectors over the continent show an increase in wind speed and a veering with time following the

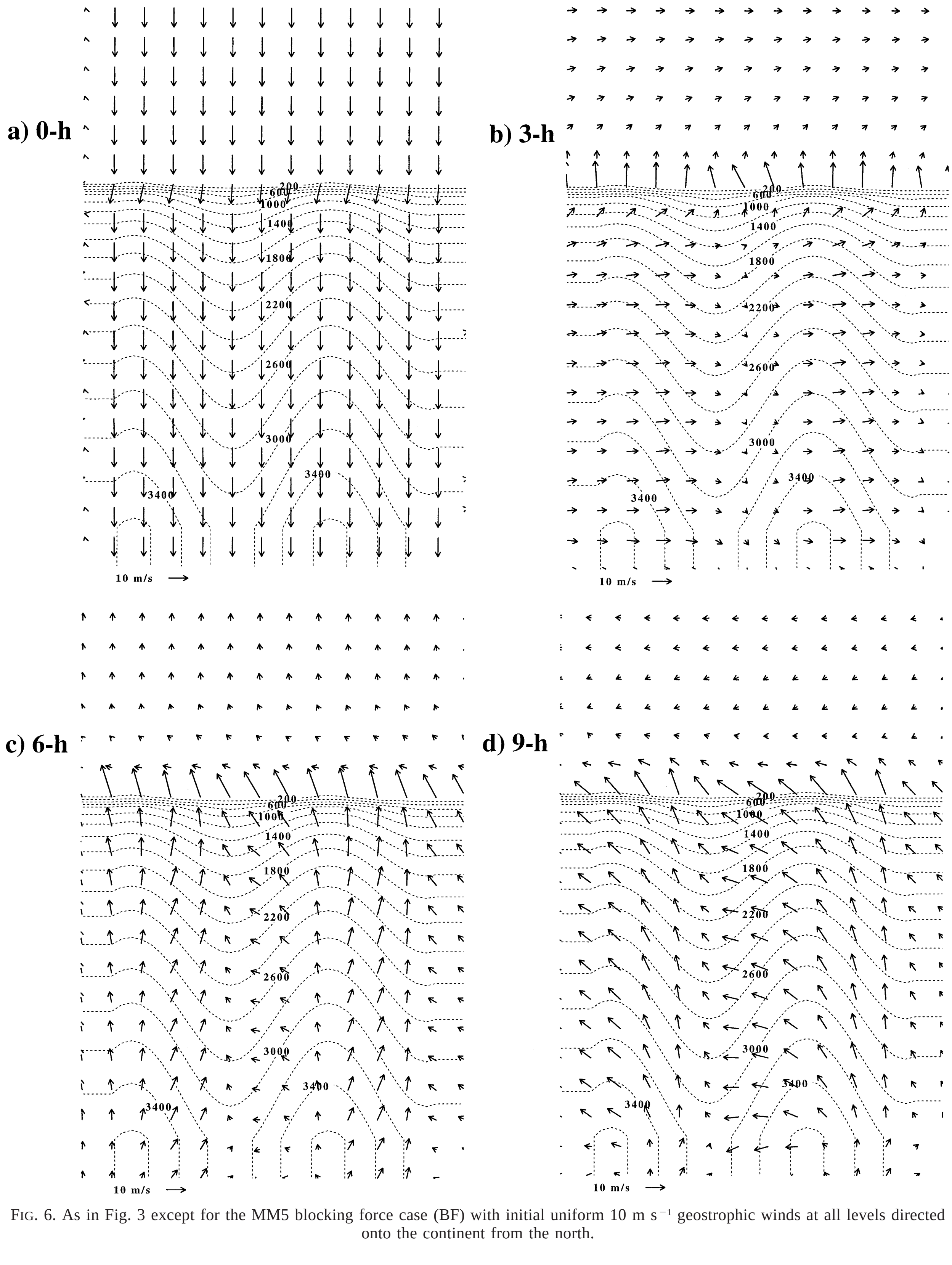

FIG. 6. As in Fig. 3 except for the MM5 blocking force case (BF) with initial uniform 10 m s^{-1} geostrophic winds at all levels directed onto the continent from the north.

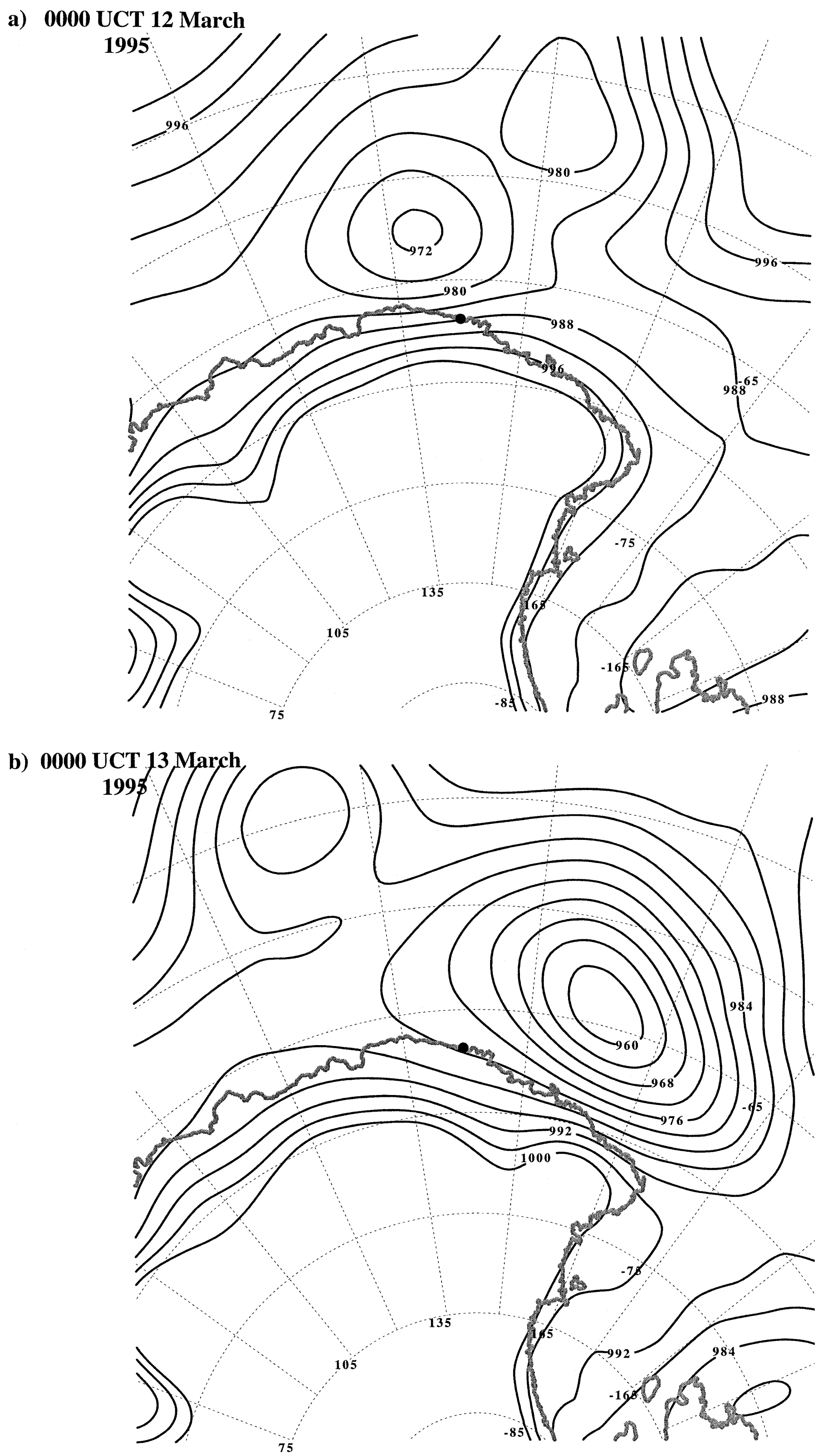

FIG. 7. Analysis of sea level pressure (hPa) for (a) 0000 UTC 12 Mar 1995 and (b) 0000 UTC 13 Mar 1995 from NCEP–NCAR reanalysis grids. Position of Cape Denison noted by dot. Analysis is deleted over Antarctic high interior since reduction to sea level pressure analysis is not valid.

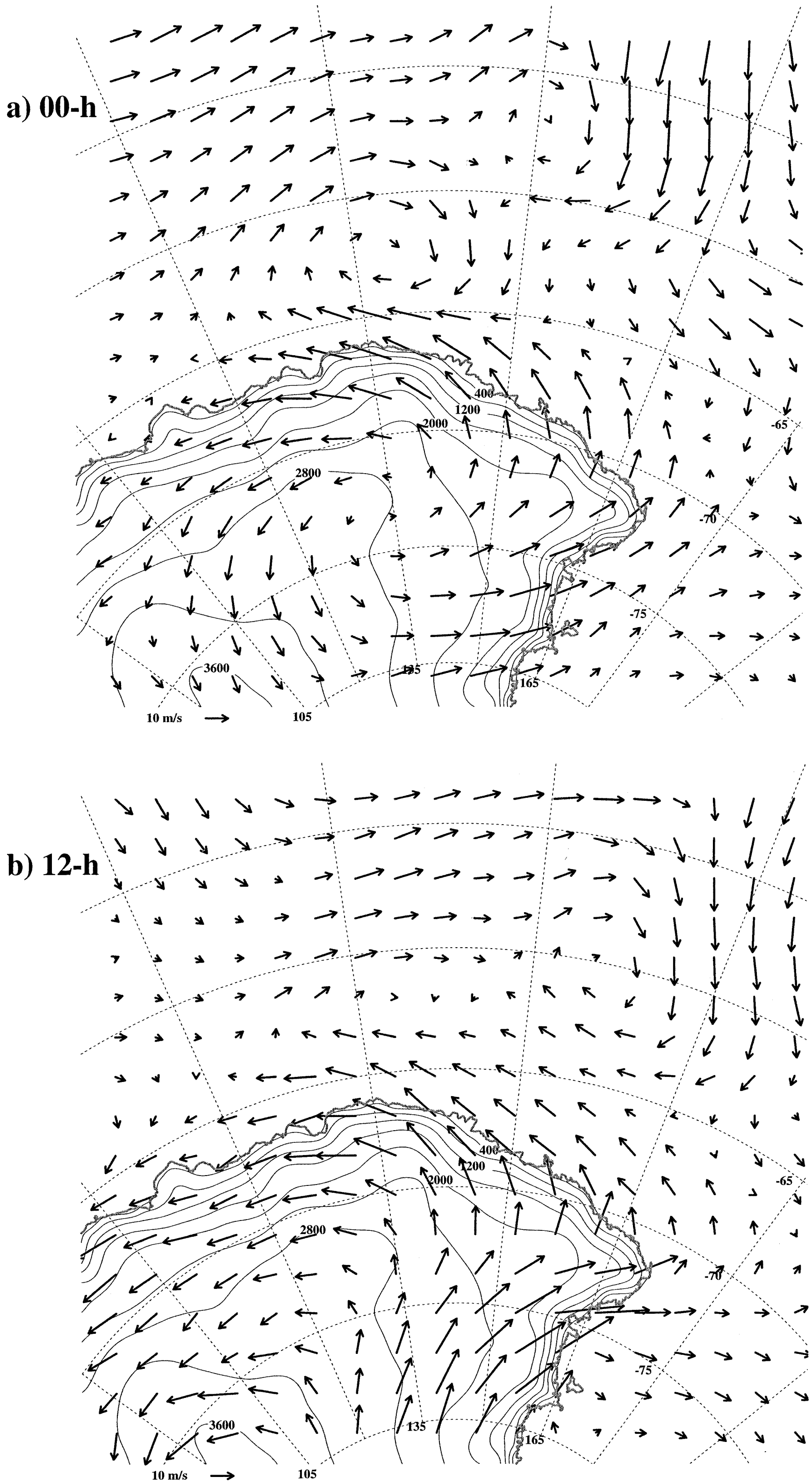

FIG. 8. MM5 simulation of wind vectors at lowest sigma level (5 m above ground) at (a) 0 (0000 UTC 12 Mar 1995), (b) 12, (c) 24, and (d) 36 h. Terrain contours (m) denoted by thin solid lines.

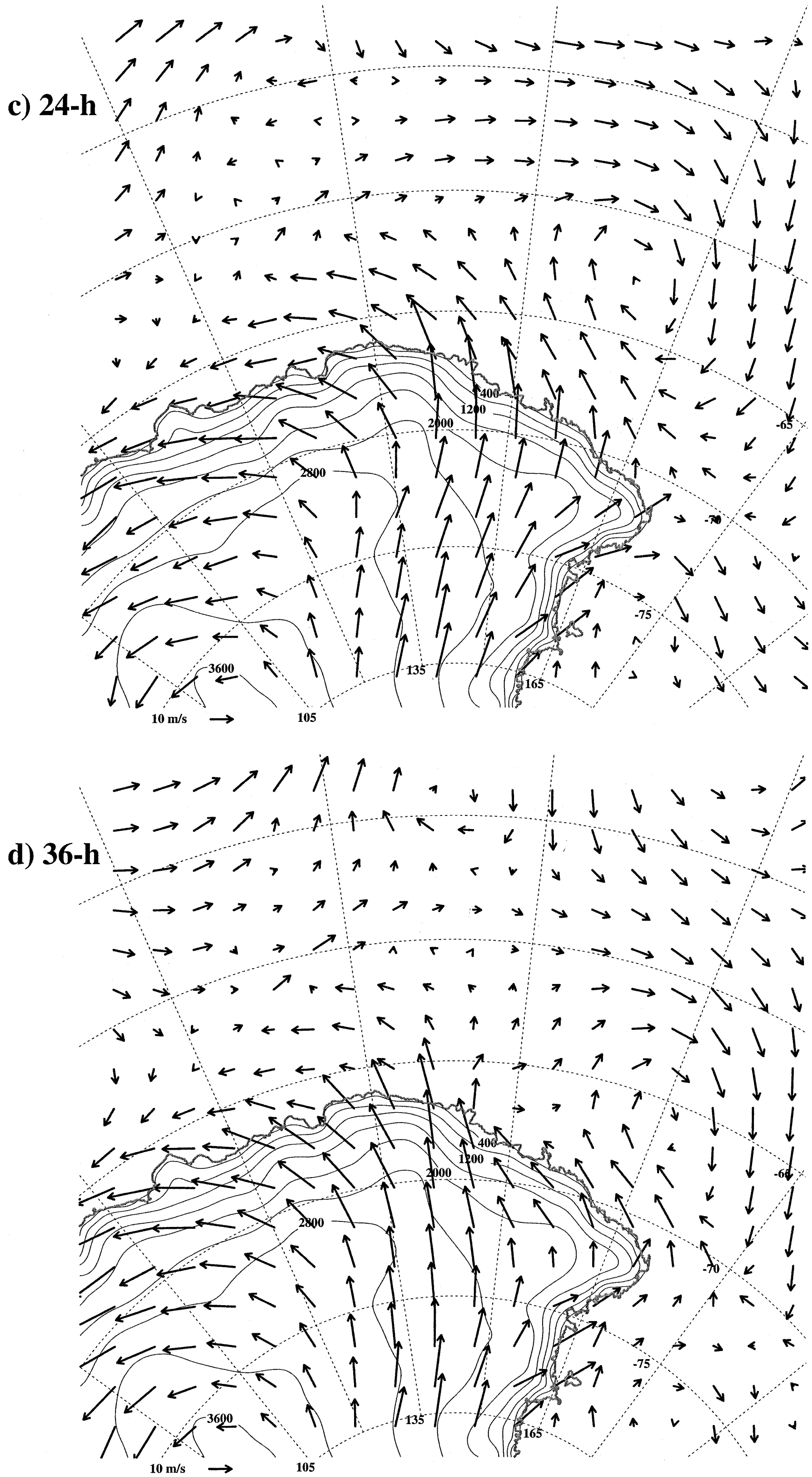

FIG. 8. (*Continued*)

progression of the cyclone, in agreement with observed trends at AWS sites. For example, wind speeds at the lowest sigma level for the grid point corresponding to Cape Denison increased during the first 24 h from 22 to 29 m s^{-1} and wind directions shifted from approximately 130° to 175°. This is in good agreement with trends shown in Fig. 2a.

Tendencies in the equations of motion in MM5 have been output to examine the forcing terms for the wind. In particular, the PGF is critical to understanding the roles played by the synoptic and katabatic components. Figure 9 illustrates the PGF from MM5 at the lowest sigma level for 12 and 36 h, corresponding to 1200 UTC on 12 and 13 March, respectively. Here the PGF is scaled by the Coriolis parameter so it has a magnitude equal to the geostrophic wind. It is apparent from Fig. 9 that, despite the rapid deepening of the cyclone during this period, the direction of the PGF over the Antarctic continent retains a close coupling to the underlying terrain. The PGF over the continent is directed down the local fall line throughout the simulation. The largest magnitudes of the PGF are found over the steep coastal section of Antarctica, which is situated at a considerable distance from the cyclone center. This implies that a pronounced adjustment has taken place between the ambient pressure field associated with the cyclone and the ice topography. Significant changes in the PGF to the north of the continent are apparent in Fig. 9 following the movement of the cyclone. Note that the magnitude of the PGF over the continent increases from 12 to 36 h adjacent to Cape Denison and south along approximately 145°E in response to the motion of the cyclone.

Estimates of the katabatic component of the PGF were made using the technique described in section 3. It was first necessary to determine the potential temperature deficit at each sigma level for each grid point. As before, it was assumed that potential temperatures in the layer from 1500 to 3000 m above the surface are representative of the ambient environment. This lower height is above the boundary layer everywhere over Antarctica in the model domain and hence is thought to be above the influence of radiative cooling of the ice slopes and katabatic wind effects. A least squares linear fit was applied to the layer and extrapolated to the surface. The difference between the model potential temperatures at each sigma level and the extrapolated ambient temperatures provides an estimate of the deficit. Terrain slopes can be determined for each grid point using the same finite-difference methods as used in MM5. Applying the first rhs term in (1), an estimate of the katabatic component of the PGF can be obtained.

Figure 10 illustrates the katabatic component of the PGF at the lowest sigma level for 12 and 36 h. Each vector is scaled by the Coriolis parameter so as to represent a geostrophic magnitude. By definition, each PGF vector is directed down the local fall line. As is obvious from Fig. 10, the katabatic component is but a fraction of the total PGF over the entire continent except for the steep coastal slopes for both periods. The katabatic component is very small at 12 h, which may be a reflection of initial conditions in part although ample time has passed from the start of the integration for katabatic components to develop. At 36 h, the katabatic component is significantly larger, especially to the west of the cyclone. This is consistent with clearing skies following passage of the cyclone, although the cause for the enhanced katabatic PGF is not known. Regardless, it is obvious that the total PGF for this case contains only a minor katabatic component and primarily is a reflection of the ambient PGF. Significant adjustment of the horizontal pressure field associated with the cyclone by the continental terrain is responsible for the enhancement of the wind. It can be concluded that the strong surface winds along the coast of Antarctica as depicted in this MM5 simulation from 12 to 13 March are not primarily katabatic in origin.

This sequence of synoptic events is repeated time and again in the records of manned stations and AWSs along the coast of Antarctica. Although the enhanced wind speeds and directions from favored topographic pathways may suggest that the winds are fundamentally katabatic, this simulation suggests that other process can act to force surface winds over Antarctica. Blocking by the Antarctic terrain and subsequent adjustment of the PGF is a likely candidate to explain the behavior of the wind field. The importance of adjustment processes at work between the Antarctic terrain and the synoptic-scale pressure field in producing the Antarctic wind field cannot be overemphasized. This topographic adjustment provides a different interpretation of the forcing of Antarctic surface winds and casts doubt on the fundamental importance of katabatic influence.

5. Summary

The directional constancy and topographic control of the Antarctic surface wind field has been largely attributed to the influence of katabatic processes. It is clear that such an interpretation cannot be used to explain the persistence of the wind regime during summer months or during situations of strong cyclone forcing. It is proposed that processes other than those resulting from katabatic forcing are active and can equally well explain the principal characteristics of the Antarctic surface wind regime throughout the year. Findings here are similar to those suggested in Parish and Cassano (2001). In that paper, it was argued that the adjustment process alone can result in wind fields similar to those observed over the Antarctic continent without requiring significant katabatic forcing.

Numerical simulations have shown that pronounced adjustments in the pressure and wind fields take place when stable air impinges on the continental orography. The Antarctic ice massif acts to block the flow of stable air toward the continent. The subsequent adjustment process results in a horizontal pressure field that is

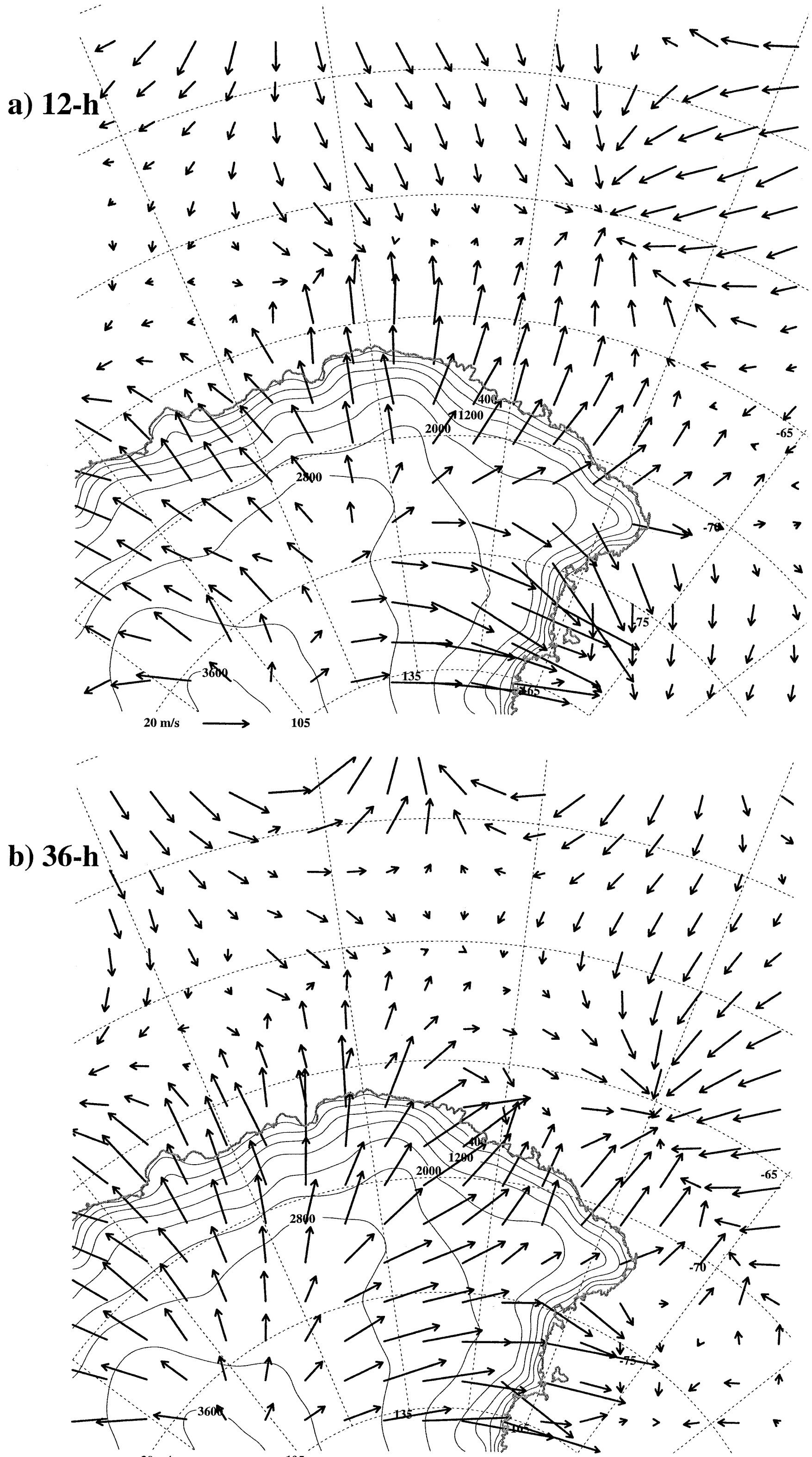

FIG. 9. As in Fig. 7 except for PGF at (a) 12 and (b) 36 h. Length of vectors corresponds to geostrophic wind magnitude (m s^{-1}).

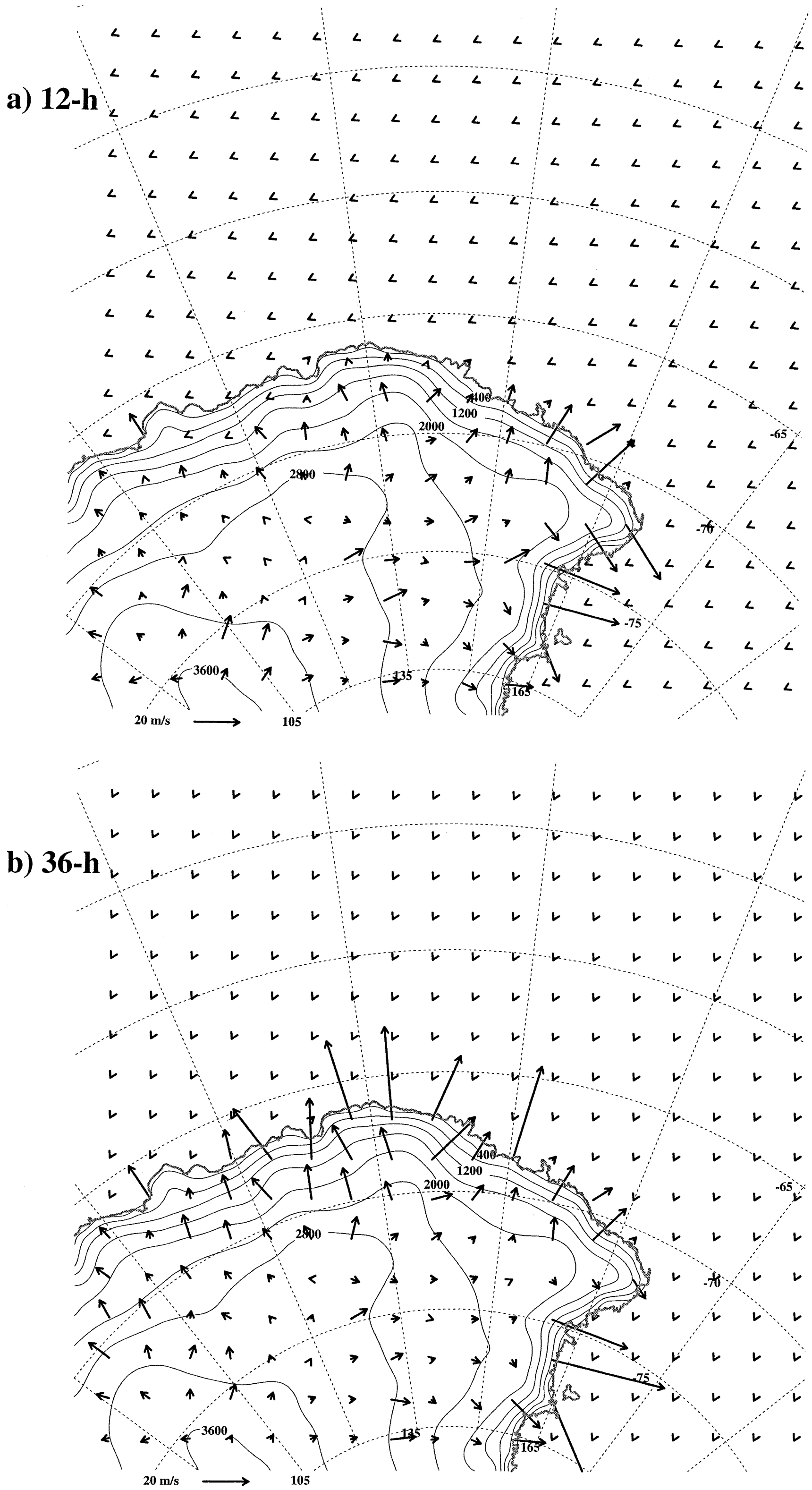

FIG. 10. As in Fig. 8 except for katabatic component of PGF at (a) 12 and (b) 36 h.

shaped by the slope and direction of the terrain. Simple numerical simulations have shown that any north–south PGF, as would be expected to exist immediately to the north of the Antarctic contintent, will result in an adjusted wind field that follows the underlying topography. Simulations have indicated that the resulting wind fields from purely katabatic processes are indistinguishable from those forced through a variety of synoptic conditions. This implies that wind direction alone is a poor indicator of katabatic activity.

Simulations of the 11–14 March 1995 case study are illustrative of the role of the adjusted ambient PGF in establishing the surface wind. Despite strong cyclonic forcing, the PGF over the continent remains directed along preferred topographic pathways. Blocking effects associated with the cyclonic circulation adjacent to the steep coastal terrain promote an adjustment over the continent. The resulting PGF over Antarctica becomes enhanced as the axis of the cyclone passes to the north. Because of the terrain adjustment, the PGF over the continent is significantly different than that found over the adjacent ocean to the north of the continent. For forecasting purposes, the Antarctic surface wind regime is a poor indicator of changing synoptic conditions. Only subtle changes in wind direction and an increase in wind speed appear to mark the passage of a cyclone center to the north. As recognized long ago, the relationship between wind and weather over the Antarctic ice sheet is considerably different than that seen in midlatitudes.

Acknowledgments. This research was funded in part by National Science Foundation Grant OPP-9725263.

REFERENCES

Ahrens, C. D., 2000: *Meteorology Today.* 6th ed. Brooks/Cole, 528 pp.

Baines, P. G., and K. Fraedrich, 1989: Topographic effects on the mean tropospheric flow patterns around Antarctica. *J. Atmos. Sci.,* **46,** 3401–3415.

Ball, F. K., 1956: The theory of strong katabatic winds. *Aust. J. Phys.,* **9,** 373–386.

——, 1960: Winds on the ice slope of Antarctica. *Antarctic Meteorology, Proceedings of the Symposium of Meldourne, 1959.* Pergamon, 9–16.

Bintanja, R., 2000: Mesoscale meteorological conditions in Dronning Maud Land, Antarctica, during summer: A qualitative analysis of forcing mechanisms. *J. Appl. Meteor.,* **39,** 2348–2370.

Cassano, J. J., and T. R. Parish, 2000: An analysis of nonhydrostatic dynamics in numerically simulated Antarctic katabatic flows. *J. Atmos. Sci.,* **57,** 891–898.

Grell, G. A., J. Dudia, and D. R. Sauffer, 1994: A description of the fifth-generation Penn State/NCAR Mesoscale Model (MM5). NCAR Tech. Note NCAR/TN-398+STR, 122 pp.

Hack, J. J., B. A. Boville, B. P. Briegleb, J. T. Kiehl, P. J. Rasch, and D. L. Williamson, 1993: Description of the NCAR Community Climate Model (CCM2). NCAR Tech. Note NCAR/TN-382+STR, 108 pp.

Hong, S.-Y., and H.-L. Pan, 1996: Nonlocal boundary layer vertical diffusion in a medium-range forecast model. *Mon. Wea. Rev.,* **124,** 2322–2339.

Huschke, R. E., Ed., 1959: *Glossary of Meteorology.* Amer. Meteor. Soc., 638 pp.

Kalnay, E., and Coauthors, 1996: The NCEP/NCAR 40-Year Reanalysis Project. *Bull. Amer. Meteor. Soc.,* **77,** 437–471.

Keller, L. M., G. A. Weidner, and C. R. Stearns, 1994: Antarctic automatic weather station data for the calendar year 1992. Dept. of Atmospheric and Oceanic Sciences, University of Wisconsin—Madison, 356 pp. [Available from Dept. of Atmospheric and Oceanic Sciences, University of Wisconsin—Madison, Madison, WI 53706.]

Kodama, Y., G. Wendler, and N. Ishikawa, 1989: The diurnal variation of the boundary layer in summer in Adélie Land, eastern Antarctica. *J. Appl. Meteor.,* **28,** 16–24.

Lettau, H. H., and W. Schwerdtfeger, 1967: Dynamics of the surface-wind regime over the interior of Antarctica. *Antarct. J. U.S.,* **2** (5), 155–158.

Lutgens, F. K., and E. J. Tarbuck, 2001: *The Atmosphere.* 8th ed. Prentice Hall, 484 pp.

Mather, K. B., and G. S. Miller, 1966: Wind drainage off the high plateau of eastern Antarctica. *Nature,* **209,** 281–284.

——, and ——, 1967: The problem of the katabatic wind on the coast of Terre Adélie. *Polar Rec.,* **13,** 425–432.

Meehl, G. A., 1991: A reexamination of the mechanism of the semiannual oscillation in the Southern Hemisphere. *J. Climate,* **4,** 911–926.

Moran, J. M., and M. D. Morgan, 1997: *Meteorology.* 5th ed. Prentice Hall, 530 pp.

Murphy, B. F., and I. Simmonds, 1993: An analysis of strong wind events simulated in a GCM near Casey in the Antarctic. *Mon. Wea. Rev.,* **121,** 522–534.

Neff, W. D., 1999: Decadal-time-scale trends and variability in the tropospheric circulation over the South Pole. *J. Geophys. Res.,* **104,** 27 217–27 251.

Parish, T. R., 1981: The katabatic winds of Cape Denison and Port Martin. *Polar Rec.,* **20,** 525–532.

——, 1982: Surface airflow over East Antarctica. *Mon. Wea. Rev.,* **110,** 84–90.

——, and D. H. Bromwich, 1987: The surface windfield over the Antarctic ice sheets. *Nature,* **328,** 51–54.

——, and K. T. Waight, 1987: The forcing of Antarctic katabatic winds. *Mon. Wea. Rev.,* **115,** 2214–2226.

——, and G. Wendler, 1991: The katabatic wind regime at Adélie Land. *Int. J. Climatol.,* **11,** 97–107.

——, and J. J. Cassano, 2001: Forcing of the wintertime Antarctic boundary layer winds from the NCEP/NCAR global reanalysis. *J. Appl. Meteor.,* **40,** 810–821.

Radok, U., 1973: On the energetics of surface winds of the Antarctic ice cap. *Energy Fluxes over Polar Surface,* WMO Tech. Note 129, World Meteorological Organization, 69–100.

Schwerdtfeger, W., 1960: The seasonal variation of the strength of the southern circumpolar vortex. *Mon. Wea. Rev.,* **88,** 203–208.

——, 1970: The climate of the Antarctic. *World Survey of Climatology,* S. Orvig, Ed., Vol. XIV, Elsevier, 253–355.

——, 1975: The effect of the Antarctic Peninsula on the temperature regime of the Weddell Sea. *Mon. Wea. Rev.,* **103,** 41–51.

——, 1984: *Weather and Climate of the Antarctic.* Elsevier, 261 pp.

Simmonds, I., 1998: The climate of the Antarctic region. *Climates of the Southern Continents: Present, Past and Future,* J. E. Hobbs, J. A. Lindesay, and H. A. Bridgman, Eds., John Wiley and Sons, 137–160.

Turner, J., G. J. Marshall, and T. A. Lachlan-Cope, 1998: Analysis of synoptic-scale low pressure systems within the Antarctic Peninsula sector of the circumpolar trough. *Int. J. Climatol.,* **18,** 253–280.

van Loon, H., 1967: The half-yearly oscillations in middle and high southern latitudes and the coreless winter. *J. Atmos. Sci.,* **24,** 472–486.

Wendler, G., and Y. Kodama, 1985: Some results of the climate of Adélie Land, eastern Antarctica. *Z. Gletscherkd. Glazialgeol.,* **21,** 319–327.